JOURNAL OF APPLIED ELECTROCHEMISTRY 19 (1989) 901–910

The solubility and electrochemistry of alkali metal oxides in the molten eutectic mixture of lithium carbonate–sodium carbonate–potassium carbonate

S. H. WHITE*, U. M. TWARDOCH

EIC Laboratories Inc., 111 Downey Street, Norwood MA 02062, USA

Received 8 November 1988; revised 6 April 1989

Metal oxides as solutes in molten electrolytes are important in metal winning as well as intermediates or reaction products in a number of new energy related technologies. The systematic behaviour of oxide ions in carbonate melts has received little attention. The results of electroanalytical measurements have shown that the solubilities of alkali metal oxides in the ternary eutectic mixture Li_2CO_3–Na_2CO_3–K_2CO_3 (43.5 : 31.5 : 25 mol %) in the temperature range 400–700° C are less than 0.5 mol %. The solubilities X (mole fraction) are given by:

$$X_{\mathrm{oxide}} = 0.0538 \exp\left[-\frac{5775}{RT}\right]$$

The oxidation reaction of oxide ions on the gold electrode produces peroxide ions. The identification of this reaction stoichiometry has enabled reliable evaluation of the diffusion coefficients of oxide ions as a function of temperature from the chronopotentiometric and voltammetric measurements. The diffusion coefficients in $\mathrm{cm^2\,s^{-1}}$ ($\times 10^6$) are expressed by:

$$D_{\mathrm{oxide}} = 0.0344 \exp\left[-\frac{15377}{RT}\right]$$

where R is expressed in cal $(\mathrm{mol\,K})^{-1}$ and T in degrees Kelvin.

1. Introduction

Molten salts, in particular alkali metal halides, nitrates, sulphates and carbonates, their respective mixtures, as well as liquid polymeric electrolytes such as alkali silicates, phosphates and borates possess unique properties which make them desirable in the development of efficient methods of materials processing and energy production [1]. Metal oxides are often intimately involved in these processes either directly as in the electrowinning of aluminium [2] and the rare earth metals [3] or indirectly, as solution contaminants, intermediates, or reaction products, from the hydrolysis of solvent mixtures during preparation [4], in the electrode reactions [5] taking place in the molten carbonate fuel cell, in magnesium production [6, 7], and in hot corrosion [8, 9] respectively. Additionally, their solution chemistry and electrochemistry is fundamental to the description of acid–base behaviour [10, 11] and in the perception of electroanalytical [12, 13] or auxiliary electrodes [14–16] in a variety of molten electrolytes. In spite of the technological and fundamental consequences for the chemistry of oxides in fused salt media, relatively little is known about their solubilities [2, 17], transport properties [5, 18] and reaction chemistry with commonly encountered species such as oxygen, carbon dioxide, water [19–21] or transition metal ions [17, 22] in most of the commonly employed electrolytes. In addition, the electrochemistry of their oxidation reactions encountered at the auxiliary anode in metal production, in reference and oxide sensitive electrodes is poorly understood [12, 13, 15–17, 19, 21, 23, 24].

Oxide ions are important species in the chemistry of molten carbonates because of their relationship to the acid/base characteristics of these melts and as reaction intermediates in the cathodic reduction of oxidant in the molten carbonate fuel cell. Information about the systematic behaviour of oxide ions in these melts is rudimentary [4, 19, 25]. This paper presents data which show that the solubilities of alkali metal oxides in the ternary eutectic mixture Li_2CO_3–Na_2CO_3–K_2CO_3 (43.5 : 31.5 : 25 mol %) in the temperature range 400 to 700° C are less than 0.5 mol %. The oxidation reaction on gold is shown to produce peroxide ions

---

* Present address: 220 Harvard Lane, Wrentham, Massachusetts 02093, USA.

0021-891X/89 $03.00 + .12

according to the reaction:

$$2O^{2-} \Leftrightarrow O_2^{2-} + 2e \qquad (1)$$

The identification of this reaction stoichiometry has enabled, for the first time, reliable evaluation of the diffusion coefficients of oxide ions as a function of temperature from the chronopotentiometric and voltammetric measurements.

2. Experimental details

2.1. *Material and solvent preparation*

The ternary alkali metal carbonate mixture composed of 43.5 mol % Li_2CO_3, 31.5 mol % Na_2CO_3, 25 mol % K_2CO_3 was used. The mixture was prepared from Fisher ACS certified alkali metal carbonates by the method described previously [25]. The purified solvent mixture and the sources of oxide, either Alfa 98% sodium oxide or Cerac 99.9% lithium oxide were handled only in the argon filled dry box (Vacuum Atmospheres). The high purity grade argon, carbon dioxide and oxygen (Airco gases) which were employed in these studies were treated additionally with molecular sieves, Sofnalite, and/or hot copper turnings, to remove traces of water, carbon dioxide or oxygen as appropriate. The premixed and analysed reference gas mixtures (66.7% CO_2–33.3% O_2 and 25% CO_2–75% O_2) were of similar high purity grade. Other gas compositions were obtained using an Airco gas mixer and the compositions were determined from the calibrated flow rates [25–27].

2.2. *Experimental apparatus*

The gas lines, vacuum system and electrochemical cells have been reported earlier [26]. Briefly, the electrochemical cell consisted of a silica tube fitted with a water cooled brass header that accommodated six Ace no. 7 threaded adaptor ports through which the various electrode assemblies and inserts were introduced. The header assembly made a vacuum tight fit (O ring seal) onto the silica envelope which was 75 mm in diameter and 30–35 cm long and closed at one end. The electrolyte was contained in either a 99.99% gold crucible for the sodium oxide containing solutions or an alumina crucible (McDanel 998 grade) for those containing lithium oxide. The cells were heated in furnaces with wire wound resistance elements either powered by two 10 ampere variacs, or a Eurotherm temperature controller/power supply. Temperature control was achieved with feedback from Chromel–Alumel thermocouples mounted close by the furnace elements. The actual solution temperatures were measured in the cell with a calibrated Chromel–Alumel thermocouple (Omega).

The counter electrode was a large 2 × 2 cm^2 flag cut from gold foil (Johnson Matthey 99.99%). The gold flag was mounted on gold wire which was sealed into an alumina capillary tube. The sheathed gold wire was attached to a silver lead wire which was enclosed in alumina tube (5 mm outside diameter) sealed with epoxy into a 20 cm length of 7 mm Pyrex tubing [26]. The assembly was mounted with a Viton O ring into an Ace no. 7 port. Working electrodes were smaller gold flags. These gold electrodes were made from electropolished foil, 0.005 mm thick. The flag, approximately 0.4 × 0.3 cm^2, was welded to a gold wire which had been sealed into alumina capillary tubing [26]. The electrode was supported in the manner described for the counter electrode.

A gas reference electrode based upon the design illustrated previously using the CO_2/O_2 gas mixtures (indicated accordingly in the subsequent figures) was employed in the carbonate solutions:

$$Au/CO_2\text{-}O_2/Li_2CO_3\text{-}Na_2CO_3\text{-}K_2CO_3 \parallel Al_2O_3 \qquad (2)$$

The electrode in this form [27] can be dismantled for cleaning and reused in subsequent experiments. A number of other inserts which included an addition tube, a thermocouple sheath and a gas inlet and outlet system [28] were also employed.

2.3. *Electrochemical techniques*

Cyclic voltammetry and current reversal chronopotentiometry were adopted to investigate the solution chemistry of alkali metal oxides in the molten carbonate. The electrochemical instrumentation was based upon an Amel 551 potentiostat modulated by a PAR 175 wave-form generator. The current or voltage transients were recorded on a Bascom Turner 8120 series microprocessor controlled recorder and stored on floppy disks for further analysis. All open circuit potentials were measured with a Data Precision 2480 digital voltmeter.

2.4. *Procedures*

The cell components which came into contact with the salt solutions were cleaned with a 50% H_2SO_4–50% HNO_3 mixture, soaked in distilled water and rinsed before drying in an oven. Each electrode assembly was evacuated on the vacuum line before use to ensure that the seals were gas tight and all moisture was removed. The assembled cell, containing the crucible was completely dried under reduced pressure before transfer into the dry-box. At this stage, the solvent mixture ($\sim$ 120 g) was introduced into the crucible which was returned to the main cell. Pellets for the addition of the alkali oxides (either Na_2O or Li_2O) were prepared and loaded into the addition tube assembly at this time. The cell was removed from the dry box into the furnace, connected on to the vacuum system and the pressure reduced to a level of about 5 microns under ambient conditions. The temperature was then raised to around 450° C before bringing the pressure to one atmosphere with argon. The melt background was evaluated using cyclic voltammetry. The appropriate experimental conditions were established in the cell and measurements commenced. For the solubility measurements, iR compensation was found unnecessary

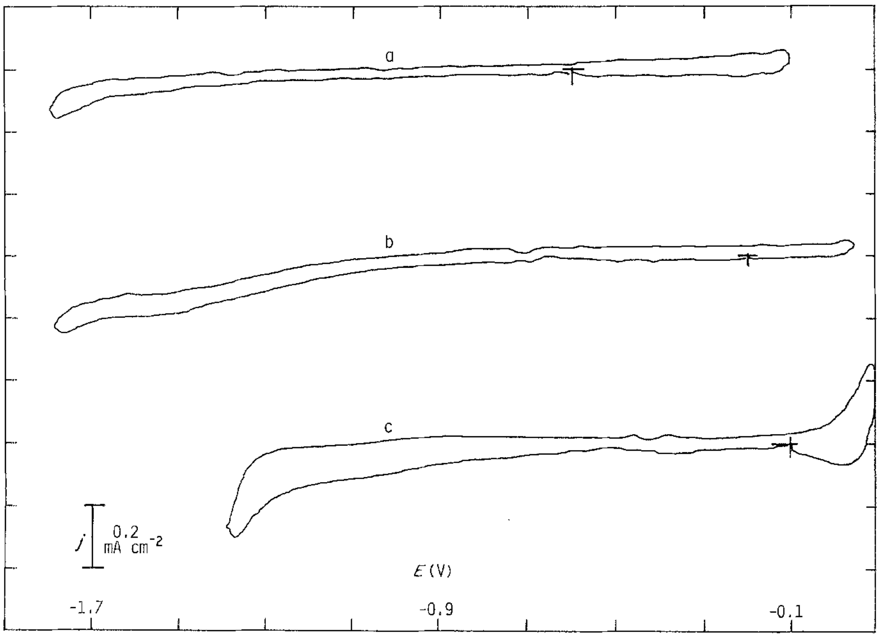

Fig. 1. Comparison of the cyclic voltammetric background responses acquired at 0.1 V s^{-1}, at a gold electrode in the ternary alkali metal carbonate eutectic mixture under different experimental conditions: a) argon atmosphere, 460° C; b) carbon dioxide atmosphere, 460° C; c) carbon dioxide atmosphere, 670° C. Reference electrode CO_2/O_2(67%–33%)/Au.

for scan rates below 1 V s^{-1}. A background correction was made for the residual amount of oxide detected in the melt. The electrode areas were determined after the experiment using the procedure of Wolfe and Caton [29].

3. Results and discussion

3.1. *Purity and thermal behaviour of the ternary alkali metal carbonate eutectic mixture*

The alkali metal carbonate source materials were of good quality, the major impurity is associated with sulphur (as sulphate) in the lithium carbonate which corresponds to a concentration in the untreated melt of about 3 millimolar. The preparative treatments adopted produced melts which had residual current densities at 0.1 V s^{-1} lower than 100 × 10^{-6} A cm^{-2} at 670° C and less than 50 × 10^{-6} A cm^{-2} at 460° C under carbon dioxide containing gases. The electrochemical window under these conditions was -1.4 V at 670° C and -1.8 V at 460° C. Figure 1 illustrates some typical residual current density profiles on gold electrodes. At 460° C, no extrinsic or intrinsic impurities were detectable under argon. However, at 660° C, under argon, an oxidation peak was detected close to the anodic limit, Fig. 2. Previous studies [30, 31] of the thermodynamic properties of these melts showed that in the absence of carbon dioxide, alkali metal carbonates become unstable as the temperature is raised above 600° C and slowly decompose to form the alkali metal oxide

$$M_2CO_3 \Leftrightarrow M_2O + CO_2 \qquad (3)$$

where the activity of metal oxide a_{M_2O} is given by:

$$a_{M_2O} = K_p[CO_2]^{-1} \qquad (4)$$

The peak observed at 660° C in the anodic scan is attributed to the oxidation of oxide ions formed by the thermal decomposition of the solvent at the highest temperature used. The identity of this peak response was confirmed by an addition of lithium oxide to the melt which caused an increase in height of the residual anodic peak, Fig. 2b. The slow initial thermal decomposition of the carbonate mixture, under flowing argon following stabilization under carbon dioxide, was observed using voltammetry and the sequence of curves is illustrated in Fig. 3. At potentials lower than -0.9 V, the presence of dissolved carbon dioxide is detected in the cathodic going sweep and its concentration decreases with time. Concurrently, the anodic peak at ~ -0.15 V increases. After several hours, changes in the concentration level of oxide are only detected by leaving the solutions for 12 or more hours between measurements. The partial pressures of carbon dioxide calculated from thermodynamic data for the temperature range 400–700° C over a melt saturated with alkali metal oxide suggest that traces of carbon dioxide in the supernatant gas would be sufficient to establish quasi-equilibrium conditions in the bulk of the melt and slow mass transport of the carbon dioxide controls the rate of decomposition consistent with the results in Fig. 3.

When the carbonate solvent was heated to only 460° C, no anodic peak due to thermal decomposition of the carbonate ion was detected under argon. Addition of sodium oxide to the melt at this temperature resulted in the appearance of an anodic peak. This demonstrates that the absence of the oxide peak is not due to the insolubility of the alkali metal oxide at this low temperature. It is concluded from these results that the thermal decomposition of the melt at 450° C is minimal, although, owing to the anodic shift of this peak with decreasing concentration, the lower limit of detection is difficult to assess.

3.2. *A study of alkali oxides in the ternary alkali metal carbonate eutectic mixture*

Preliminary studies were made to establish the necessary

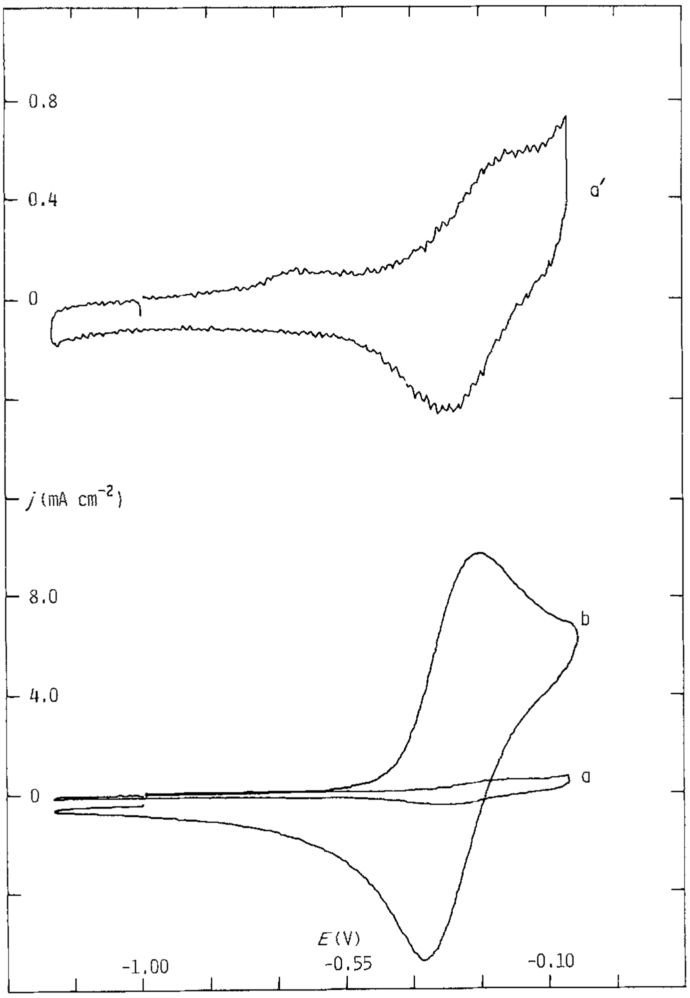

Fig. 2. The detection and identification of oxide formation from the thermal decomposition of the Li_2CO_3–Na_2CO_3–K_2CO_3 at 670° C under argon by cyclic voltammetry. Reference electrode CO_2/O_2(25%–75%)/Au. a) voltammogram acquired at 1 V s^{-1} for a gold electrode after exposing the melt to argon for two h. b) voltammogram acquired at the same electrode after a pilot addition of lithium oxide (8.3×10^{-3} mol kg^{-1}) to the melt. a′) voltammogram a) scaled 10 × to illustrate the existence of an adsorption prepeak at the lower concentration of oxide.

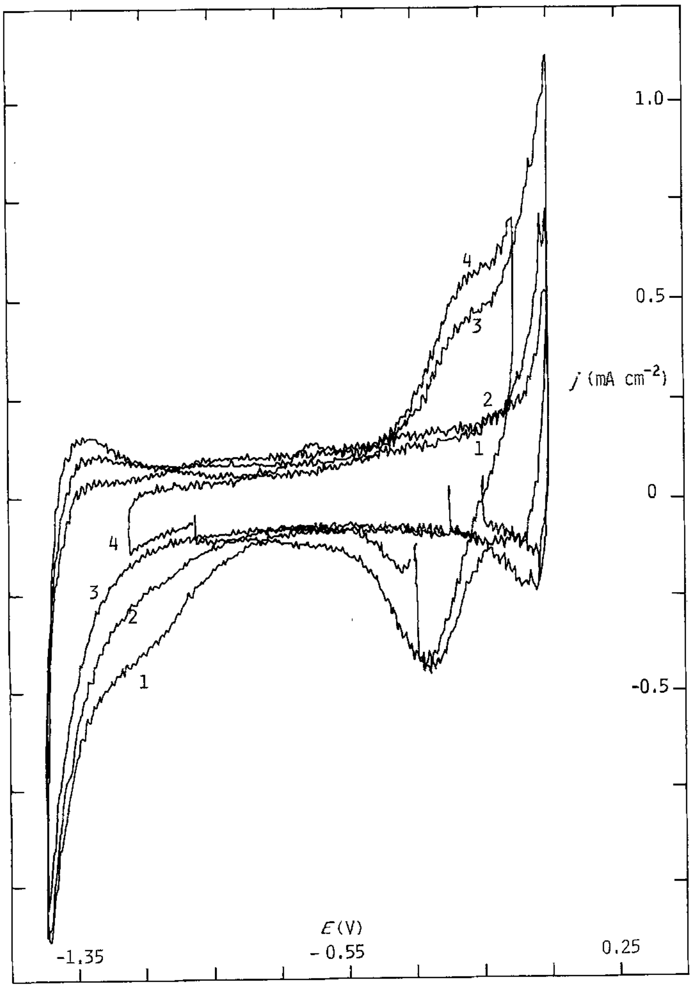

Fig. 3. The slow thermal decomposition at 670° C of pure Li_2CO_3–Na_2CO_3–K_2CO_3 mixture under a flowing atmosphere of argon as delineated by cyclic voltammetry. Reference electrode CO_2/O_2(25%–75%)/Au. Voltammograms acquired for a gold electrode at 1 V s^{-1} under the following conditions: 1) under an atmosphere of CO_2–argon (1 : 1), $t = 0$; 2) 100% argon, t = 20 min; 3) 100% argon, t = 85 min; 4) 100% argon, t = 120 min.

conditions for the electroanalysis of oxide ions in the carbonate eutectic melt. The results of these measurements characterized the small thermal decomposition of the solvent at temperatures above 550° C (see above). The pilot additions of alkali metal oxides qualitatively confirmed the electroactivity of oxide, see Fig. 2. The quantitative interpretation of the measurements, suggested that alkali metal oxides have a limited solubility in this ternary alkali metal carbonate eutectic mixture.

The solubility of the alkali metal oxide can be determined voltammetrically or chronopotentiometrically without recourse to detailed knowledge of the electrode reactions, by calibrating the electrochemical response functions at concentrations below those necessary to saturate the solution. This requires that the response function is linear in concentration and this will be true in the absence of adsorption and/or higher order coupled chemical reactions. The measured $i\tau^{1/2}$ and $i_p v^{-1/2}$ for the unsaturated solutions used indicate that in the applied current density and scan rate ranges employed the processes are controlled by diffusion. Consequently, the solubilities of the alkali metal oxide were obtained from the following sequence of measurements.

Initially, an estimate of the saturation concentration of lithium oxide was obtained at the lowest temperature for which solubility data were to be determined, by adding small increments of alkali oxide until the electrochemical responses were constant. An amount less than this estimate was added to pure solvent at 670° C. Cyclic voltammetric and chronopotentiometric measurements for the oxidation of this known addition of oxide were made over a wide range of scan rates and current densities at this and at a series of lower temperatures. A second set of measurements were then made in which the additions were in excess of the expected solubility at the highest temperature. That the solubility limit indeed had been reached was confirmed by adding a further quantity of the alkali metal oxide at the highest temperature. Saturation conditions were established at each temperature by leaving the solution for at least 12 h (overnight) before making measurements. The constancy and reproducibility of the cyclic voltammetric and chronopotentiometric responses was evidence that the solutions were saturated. Data were also obtained for saturating additions of sodium oxide and these were consistent with the data for saturated solutions of lithium oxide.

Representative chronopotentiograms and cyclic voltammograms at 475° C and 680° C for unsaturated and saturated solutions of alkali metal oxide in the molten alkali metal carbonate are shown in Figs 4 and 5. Chronopotentiometric data and cyclic voltammetric data in the scan rate range 0.05 to 5.0 V s^{-1} are presented in Tables 1 and 2. Plots of i_p versus $v^{1/2}$ and $\tau^{1/2}$ versus $1/i$ are linear for both the unsaturated and

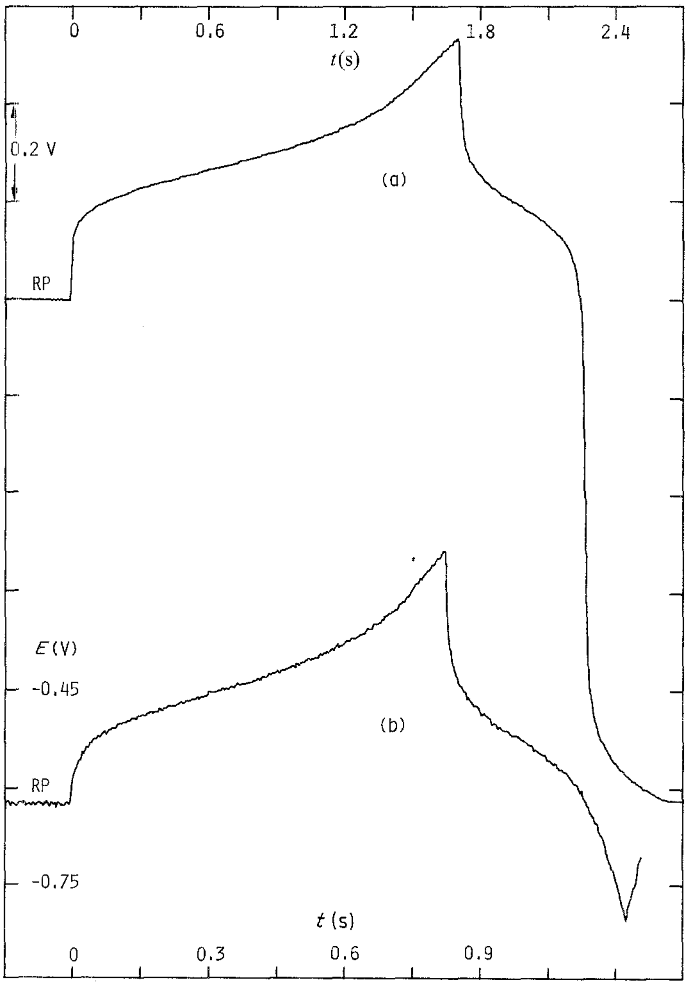

Fig. 4. Representative chronopotentiograms acquired at gold electrodes in the Li_2CO_3–Na_2CO_3–K_2CO_3 eutectic mixture containing added alkali metal oxide as a) Na_2O satuarated solution and b) Li_2O 8.78 × 10^{-3} mol kg^{-1}. The conditions were: a) 680° C, electrode area 0.48 cm^2 and an applied current density of 12.5 mA cm^{-2}, gold quasi-reference electrode; and b) 475° C, electrode area 0.52 cm^2 and an applied current density of 2.31 mA cm^{-2}. Reference electrode CO_2/O_2(25%–75%)/Au.

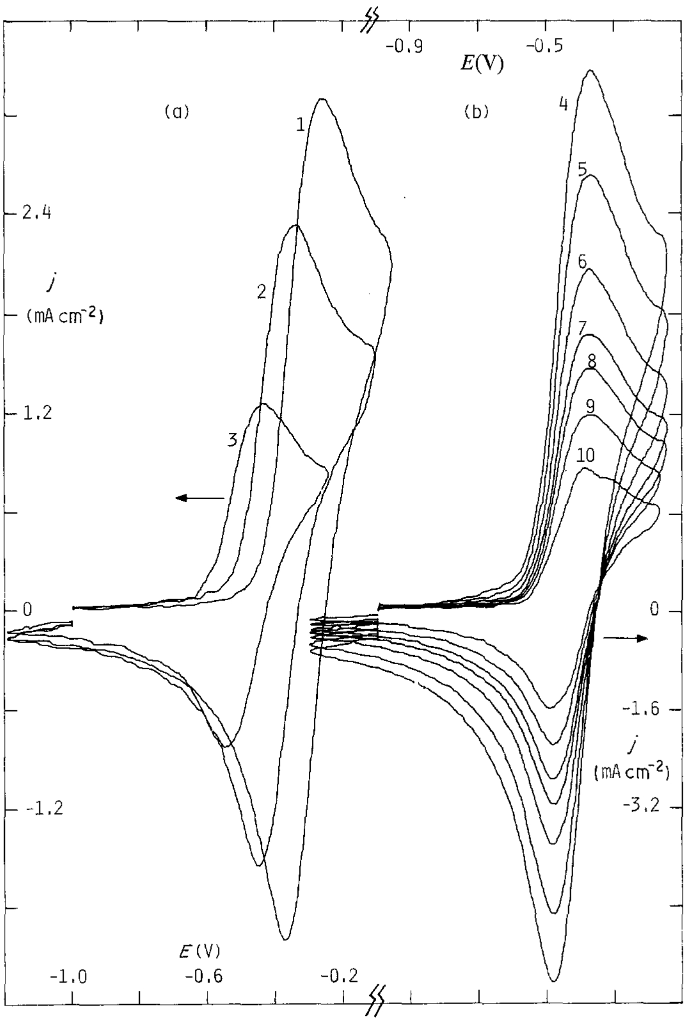

Fig. 5. Representative cyclic voltammograms for oxide ion oxidation acquired for a gold electrode in Li_2CO_3–Na_2CO_3–K_2CO_3 solutions: a) unsaturated (8.78×10^{-3} mol kg^{-1} lithium oxide) at three different temperatures and a scan rate of 0.10 V s^{-1}, b) saturated at 566° C as a function of scan rate. 1) 670° C; 2) 580° C; 3) 475° C; 4) 0.75 V s^{-1}; 5) 0.50 V s^{-1}; 6) 0.30 V s^{-1}; 7) 0.20 V s^{-1}; 8) 0.15 V s^{-1}; 9) 0.10 V s^{-1}; 10) 0.05 V s^{-1}. Reference electrode CO_2/O_2(25%–75%)/Au.

saturated solution data at temperatures between 448 and 675° C, (Figs 6 to 9). A consideration of these results and the associated potential data shows that the oxidation of oxide ions under the experimental conditions is controlled primarily by mass transport. The data are thus suitable for electroanalytical purposes.

Table 1. Chronopotentimetric data for unsaturated solutions of Li_2O dissolved in the ternary alkali metal carbonate solvent

t (° C)	i (A)	τ (s)	i $\tau^{1/2}$ ($A s^{1/2}$)	τ^b/τ^f	$E_{\tau/4}$ (V)
670	0.0060	0.124	0.00211	0.352	−0.315
670	0.0050	0.180	0.00212	0.357	−0.310
670	0.0040	0.304	0.00221	0.333	−0.310
670	0.0035	0.345	0.00206	0.334	−0.305
670	0.0030	0.525	0.00217	0.342	−0.315
670	0.0025	0.690	0.00208	0.355	−0.310
670	0.0020	1.050	0.00205	0.343	−0.315
670	0.0015	1.868	0.00205	0.336	−0.310
580	0.0040	0.143	0.00155	0.320	−0.390
580	0.0035	0.183	0.00150	0.360	−0.400
580	0.0030	0.308	0.00166	0.315	−0.390
580	0.0025	0.366	0.00151	0.348	−0.400
580	0.0020	0.593	0.00154	–	−0.395
580	0.0015	1.038	0.00153	0.311	−0.390
475	0.0020	0.161	0.000803	0.314	−0.490
475	0.0018	0.199	0.000803	0.327	−0.490
475	0.0016	0.248	0.000797	0.395	−0.495
475	0.0010	0.315	0.000786	0.368	−0.495
475	0.0010	0.405	0.000764	0.411	−0.450
475	0.0010	0.645	0.000803	0.363	−0.490

The solubility of the alkali metal oxide was calculated from the data in the following manner. The peak current (i_p) response in voltammetry is given by

$$i_p = \frac{nFmCA\{nFDv\}^{1/2}\chi}{\{RT\}^{1/2}} \tag{5}$$

and the chronopotentiometric transition time τ is given by

$$\tau^{1/2} = \frac{\pi^{1/2}nFmCAD^{1/2}}{2i} \tag{6}$$

where, A is the electrode area in cm^2, v is the scan rate in V s^{-1}, C is the depolarizer concentration in mol cm^{-3}, D is the diffusion coefficient of the depolarizer in cm^2 s^{-1}, and i is the current in amperes. χ, a function of (at), where $a = nFv/RT$ for a fast charge transfer reaction, and m, a stoichiometric factor, are dependent on the reaction mechanism. The difficulty created by the model dependence of χ is avoided by recalling that the diffusion coefficient can be expressed as a function of temperature in Arrhenius form for simple liquids [32] by

$$D = D_0 \exp\left\{\frac{-\Delta E}{RT}\right\} \tag{7}$$

Table 2. Cyclic voltammetric data for unsaturated solutions of Li_2O dissolved in the ternary alkali metal carbonate solvent

t (°C)	v ($V s^{-1}$)	i_p (A)	$i_p v^{1/2}$ ($A V^{-1/2} s^{1/2}$)	i_p^b/i_p^f	E_p^a (V)	E_p^c (V)	$E_{p/2}$ (V)
670	0.05	0.00114	0.00511	1.11	−0.260	−0.360	−0.365
670	0.1	0.00161	0.00510	1.07	−0.260	−0.365	−0.365
670	0.2	0.00226	0.00506	1.11	−0.255	−0.365	−0.360
670	0.5	0.00359	0.00508	1.11	−0.260	−0.370	−0.360
670	1.0	0.00503	0.00504	1.13	−0.260	−0.375	−0.365
670	2.0	0.00694	0.00490	1.14	−0.250	−0.380	−0.365
670	5.0	0.01125	0.00503	1.15	−0.255	−0.385	−0.360
580	0.05	0.00084	0.00377	1.08	−0.350	−0.440	−0.445
580	0.1	0.00121	0.00384	1.07	−0.345	−0.445	−0.450
580	0.2	0.00171	0.00382	1.09	−0.355	−0.455	−0.445
580	0.5	0.00269	0.00380	1.10	−0.350	−0.450	−0.445
580	1.0	0.00379	0.00379	1.11	−0.350	−0.445	−0.445
580	2.0	0.00523	0.00370	1.15	−0.340	−0.445	−0.445
475	0.05	0.00047	0.00209	1.07	−0.435	−0.540	−0.530
475	0.1	0.00065	0.00206	1.06	−0.440	−0.540	−0.535
475	0.2	0.00094	0.00211	1.06	−0.440	−0.535	−0.535
475	0.5	0.00145	0.00205	1.12	−0.440	−0.545	−0.535
475	1.0	0.00202	0.00202	1.16	−0.440	−0.540	−0.535

Combining Equations 5 and 7 and taking logarithms, the equation

$$\ln \frac{j_p T^{1/2}}{C v^{1/2}} = \alpha_{cv} - \frac{\beta}{T} \qquad (8)$$

is obtained, where j_p is the peak current density, β depends upon the activation energy for diffusion and α_{cv} is a constant containing χ and m. Although the chronopotentiometric analysis does not contain a model dependent factor such as χ, m is unknown, *a priori*, and the analysis was performed by the same method using, in this case

$$\ln \frac{j\tau^{1/2}}{C} = \alpha_{cp} - \frac{\beta}{T} \qquad (9)$$

The experimental data are summarized in Tables 1 to 3. Plotting the appropriate left hand terms versus $1/T$ for the voltammetric and chronopotentiometric

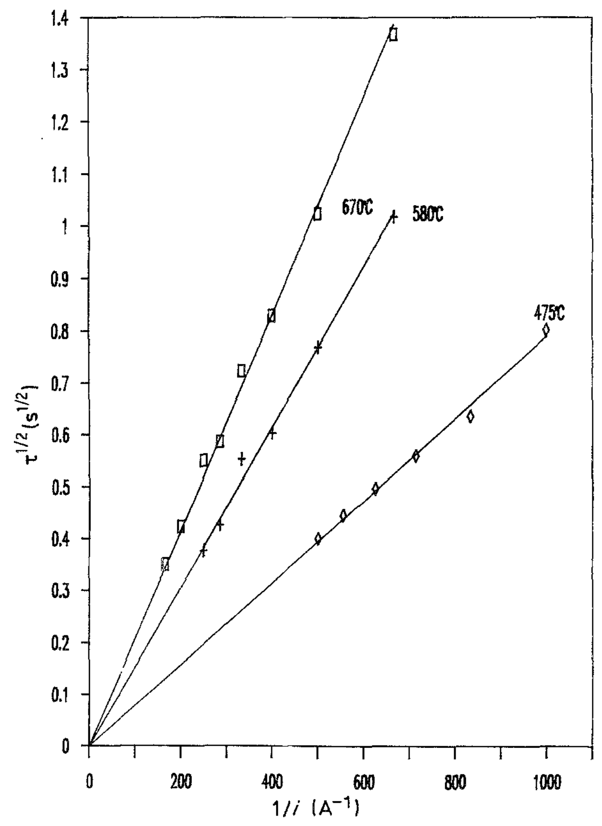

Fig. 6. Plots of $\tau^{1/2}$ against $1/i$ for the oxidation of oxide ions in unsaturated solutions at the three temperatures shown. The solid lines are the linear regression fits to the points.

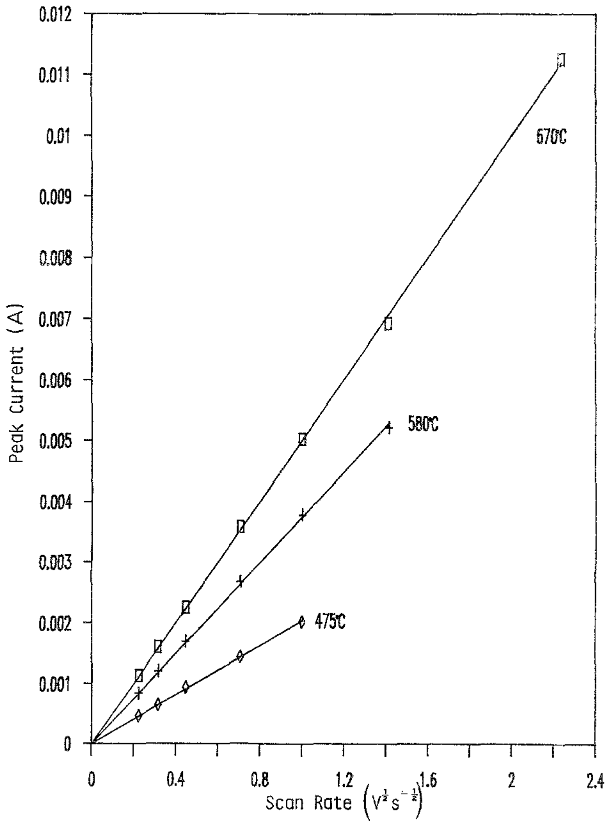

Fig. 7. Plots of i_p against $v^{1/2}$ for the oxidation of oxide ions in unsaturated solutions at the three temperatures shown. The solid lines are the linear regression fits to the points.

Table 3. Voltammetric and chronopotentimetric data for unsaturated solutions of Li_2O in the ternary alkali metal carbonate eutectic mixture

t (°C)	ϱ (g cm^{-3})	10^6 C (mol cm^{-3})	$j\tau^{1/2}$ (A cm^{-2} s$^{1/2}$)	$j_p v^{-1/2}$ (A cm^{-2} V$^{-1/2}$ s$^{1/2}$)
670	2.000	17.56	0.00404	0.00967
580	2.048	17.98	0.00302	0.00721
475	2.106	18.49	0.00152	0.00385

data obtained for the unsaturated solutions gave the following results:

$$\ln \frac{j_p T^{1/2}}{C v^{1/2}} = 14.004 - \frac{3995.4}{T} \quad (10)$$

$$\ln \frac{j\tau^{1/2}}{C} = 9.481 - \frac{3771.5}{T} \quad (11)$$

At each temperature for the solutions which were saturated, the measured $\{j_p T^{1/2}/Cv^{1/2}\}$ and $\{j\tau^{1/2}/C\}$ were combined with those calculated from the experimental values of T used and Equations 10 and 11, to determine the saturation concentrations at each temperature. The experimental data and the derived solubilities are presented in Table 4.

The two sets of solubility data are plotted as a function of temperature in Fig. 10. The data, fitted by a linear regression analysis, are expressed by

$$\ln C(\text{molal}) = -0.6207 - \frac{2906.7}{T(\text{K})} \quad (12)$$

or as

$$X_{\text{oxide}} = 0.0538 \exp\left[-\frac{5775}{RT}\right] \quad (13)$$

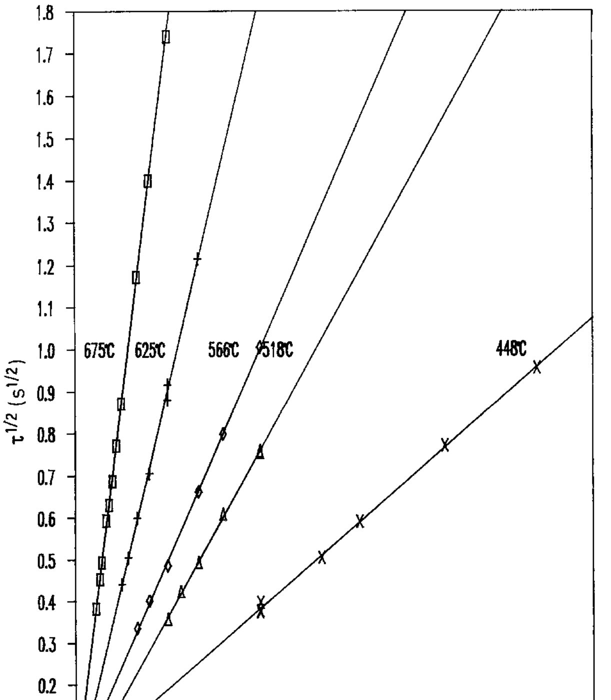

Fig. 8. Plots of $\tau^{1/2}$ against $1/i$ for the oxidation of oxide ions in saturated solutions at the temperatures shown. The solid lines are the linear regression fits to the points.

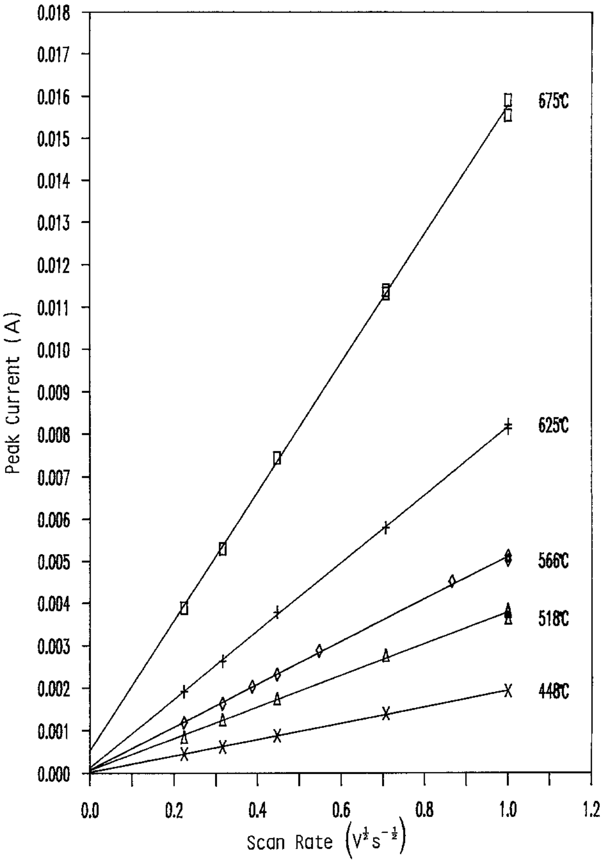

Fig. 9. Plots of i_p against $v^{1/2}$ for the oxidation of oxide ions in saturated solutions at the temperatures shown. The solid lines are the linear regression fits to the points.

The heat of solution for the dissolution of alkali metal oxide in the ternary carbonate solvent was obtained from the slope and is 5.8 ± 0.5 kcal mol^{-1}.

3.3. *Some results for the electro-oxidation of oxide ions in the ternary alkali metal carbonate eutectic solution*

The data shown in Tables 1 and 2 are now examined in more detail to establish the reaction for the anodic oxidation of oxide ions in the ternary carbonate melt. The plots of $\tau^{1/2}$ against $1/i$ and i_p against $v^{1/2}$ (Figs 6 and 7) are linear at each temperature, in accord with the Sand and Randles Sevcik Equations 5 and 6 respectively. The more sensitive tests of plotting $j\tau^{1/2}$ against j and $j_p v^{1/2}$ against v show no deviations within the range of current densities or scan rates (< 1 V s^{-1}) used, see Tables 1 and 2. At higher scan rates and shorter transition times than those discussed here evidence of surface processes coupled to the oxidation have been reported [33], (see also Fig. 2a) and these will be discussed in detail in a forthcoming paper.

The peak potential for the oxidation of oxide ions shifts anodically with decreasing concentration, Fig. 2. These results, taken in concert, indicate that the oxidation reaction is non-unitarian in its stoichiometry

Table 4. Cyclic voltammetric and chronopotentiometric data and the derived solubilities of Li_2O in the ternary alkali metal carbonate eutectic mixture

t (°C)	ϱ (g cm^{-3})	$j_p v^{-1/2}$ (A cm^{-2} V$^{-1/2}$ s$^{1/2}$)	10^5, Solubility (mol cm^{-3})	$j\tau^{1/2}$ (A cm^{-2} s$^{1/2}$)	10^5, Solubility (mol cm^{-3})
Lithium oxide					
675	1.997	0.0302	5.20	0.0135	5.49
664	2.003	0.0314	5.66	0.0133	5.66
625	2.024	0.0156	3.32	0.0070	3.57
566	2.056	0.0098	2.74	0.0039	2.63
518	2.082	0.0074	2.68	0.0029	2.63
465	2.111	0.0050	2.53	0.0021	2.63
448	2.120	0.0037	2.12	0.0015	2.10
Sodium oxide					
680	1.994	0.0344	5.82	0.0143	5.70
500	2.092	0.0064	2.60	0.0025	2.55
450	2.119	0.0036	2.00	0.0015	2.15

[34], i.e.

$$p\mathrm{Red} \Leftrightarrow q\mathrm{Ox} + ne \qquad (14)$$

The half peak width, $E_p - E_{p/2}$, the peak separation $E_p^a - E_p^c$ and the Tomes criterion $E_{3\tau/4} - E_{\tau/4}$ are compared with the theoretical values for $n = 2$ predicted [34] for Reaction 14 in Table 5. For the cyclic voltammetric data, the agreement of the results with those predicted for the potential criteria for the diffusion controlled reaction:

$$2\mathrm{O}^{2-} \Leftrightarrow \mathrm{O}_2^{2-} + 2\mathrm{e} \qquad (15)$$

is generally within experimental error. The experimental ratios of i_p^b/i_p^f, measured by Nicholson's method [35], also support this overall reaction. The agreement for the chronopotentiometric criterion $E_{3\tau/4} - E_{\tau/4}$ is less satisfactory. The coincidence of the reverse cathodic peak potential at 660° C with that of the reduction peak observed under an oxygen containing atmosphere (which was interpreted [25] as due to the reduction of peroxide ions) suggests that the major product of the oxidation reaction is peroxide ion, and is thus consistent with Reaction 15.

Since the anodic oxidation of oxide ions takes place by the Reaction 15 then the value of χ is known [33]. Thus, taking the factor $m = 1/2$, the diffusion coefficient for oxide ions can be calculated from the cyclic voltammetric and chronopotentiometric data for the additions of lithium oxide in the unsaturated solutions. The diffusion coefficients are presented in Table 6. The temperature dependence of the diffusion coefficient is given as the regression line for the two sets of data by

$$\ln D = -3.369 - \frac{7739}{T\,(\mathrm{K})} \qquad (16)$$

or

$$D_{\mathrm{oxide}} = 0.0344 \exp\left[-\frac{15377}{RT}\right] \qquad (17)$$

where D is in cm^2 s^{-1} ($\times 10^6$). The activation energy for diffusion of oxide ions is 15.4 ± 1 5 kcal mol^{-1}. The good agreement between the diffusion coefficients measured by cyclic voltammetry with those from chronopotentiometry suggest that in the range of scan rates selected the overall reaction is that written in Equation 15.

The diffusion coefficient measured for the oxide ion in the ternary carbonate melt at 670° C is of the same magnitude as that reported by earlier workers [36, 37] for the carbonate ion in the different carbonate mix-

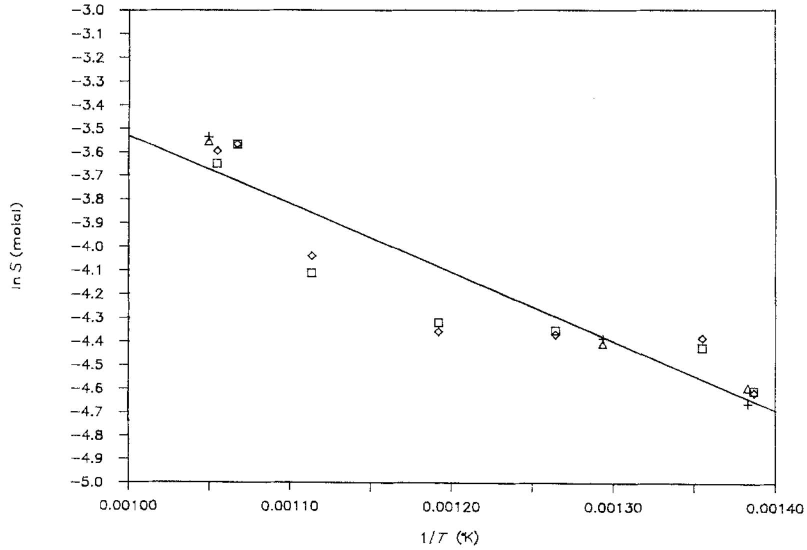

Fig. 10. Solubility of alkali metal oxides as a function of temperature in the Li_2CO_3-Na_2CO_3-K_2CO_3; Symbols: □, from CV data for Li_2O; +, from CV data for Na_2O; ◇, from CP data for Li_2O; △, from CP data for Na_2O.

Table 5. Comparison of theoretical and experimental potential functions for chronopotentiometric and cycle voltammetric data for the oxidation of oxide ions in the ternary alkali metal carbonate eutectic mixture

t (°C)	Exp.	Theory	Exp.	Theory	Exp.	Theory
	$E_p^a - E_p^c$ (mV)	3.42RT/2F (mV)	$E_p^a - E_{p/2}^a$ (mV)	3.17RT/2F (mV)	$E_{3\tau/4} - E_{\tau/4}$ (mV)	3.18RT/2F (mV)
448	116 ± 5	106	106 ± 6	98	76 ± 5	99
465	112 ± 3	108	104 ± 4	100	80 ± 4	101
475	101 ± 4	110	96 ± 4	102	76 ± 3	102
518	115 ± 10	116	105 ± 6	108	82 ± 8	108
566	102 ± 4	123	98 ± 6	114	85 ± 4	115
581	96 ± 5	125	96 ± 5	116	81 ± 4	117
625	116 ± 5	132	109 ± 7	122	85 ± 4	123
669	110 ± 7	138	105 ± 3	128	78 ± 5	129
675	154 ± 6	139	122 ± 9	129	94 ± 4	130

Table 6. The solubility of alkali oxide and the diffusion coefficients of oxide ion at different temperatures in the molten alkali metal carbonate ternary eutectic

t (°C)	Alkali oxide solubility (mol dm^{-3})	$10^6 \times D$ (cm^2 s^{-1})
670	0.049	9.4
580	0.036	4.0
475	0.023	1.1

tures at 700° C. The earlier diffusion coefficient for oxide reported by the authors [25] was subject to considerable errors in view of the estimated concentrations and the present result is to be preferred. The activation energy for diffusion of oxide is somewhat greater than those reported for self diffusion of alkali metal ions in the carbonates and considerably greater than those reported for ionic diffusion in alkali halide and nitrate melts [36–40].

The limited solubility of the alkali metal oxide in the ternary carbonate eutectic mixture is in contrast to the solubilities of oxide in the LiC–KCl melt [17]. The consequences of the low solubility of these oxides and the alkali hydroxide [26, 27] in the operation of the molten carbonate fuel cell and corresponding modelling studies have yet to be fully recognized.

References

[1] D. G. Lovering (ed.), 'Molten Salt Technology' Plenum Press (1982).

[2] K. Grjotheim, C. Krohn, M. Malinovsky, K. Matiasovsky and J. Thonstad, 'Aluminium Electrolysis; Fundamentals of the Hall–Heroult Process', 2nd edn, Aluminium-Verlag, Dusseldorf (1982).

[3] A. Mitchell and B. Thomas in 'Proc. Int. Symp. Molten Salts', (edited by M. Blander *et al.*) ECS PV 87-7, p. 863.

[4] S. H. White in 'Ionic Liquids', (edited by D. Inman and D. J. Lovering), Plenum, (1981) p. 185.

[5] J. R. Selman and H. C. Maru in 'Advances in Molten Salt Chemistry', Vol. 4 (edited by G. Mamantov and J. Braunstein), Plenum N.Y. (1981) p. 159.

[6] G. J. Kipouros and D. R. Sadoway, in 'Advances in Molten Salt Chemistry', Vol. 6 (edited by G. Mamantov and J. Braunstein), Elsevier (1987).

[7] Z. Yueqiang and L. Qingfu in 'Proc Int. Symp. Molten Salts', (edited by M. Blander *et al.*) ECS PV 87-7, p. 758.

[8] A. Rahmel in 'Molten Salt Technology', (edited by D. G. Lovering), Plenum Press, (1982).

[9] B. W. Burrows and G. J. Hills, *J. Inst. Fuels* (1966) 168.

[10] H. Lux, *Z. Elektrochem.* **45** (1939) 303.

[11] M. D. Ingram and G. J. Janz, *Electrochim. Acta* **10** (1965) 783.

[12] C. A. Melendres, J. P. Ackerman and R. K. Steunenberg in 'Proc. Int. Symp. Molten Salts', (edited by J. Braunstein *et al.*) ECS, (1976) p. 575.

[13] Y. Kanzaki and M. Takahashi, *J. Electroanal. Chem.* **58** (1975) 339.

[14] F. Lantelme, D. Damianacos and J. Chevalet, *Electrochim. Acta* **23** (1978) 717.

[15] D. Damianacos, F. Lantelme and M. Chemla, *Electrochim. Acta* **28** (1983) 217.

[16] S. Jarek and J. Thonstad, *J. Electrochem. Soc.* **134** (1987) 856.

[17] G. Delarue, *J. Electroanal. Chem.* **1** (1959) 13, 285.

[18] I. Uchida and S. Toshima, *J. Appl. Electrochem.* **9** (1979) 647.

[19] S. H. White and U. M. Twardoch, Final Report for GRI Contract No. 5081-360-0519 (1984).

[20] P. G. Zambonin and J. Jordan, *J. Am. Chem. Soc.* **91** (1969) 2225.

[21] A. A. El Hosary, D. H. Kerridge and A. M. Shams El Din, in 'Ionic Liquids', (edited by D. Inman and D. J. Lovering) Plenum (1981) p. 339.

[22] P. Mergault, *Compt. Rend.* **240** (1955) 864; **241** (1955) 1568, 1755.

[23] D. Inman and M. J. Weaver, *J. Electroanal. Chem.* **51** (1974) 45.

[24] N. S. Wrench and D. Inman, *J. Electroanal. Chem.* **17** (1968) 319.

[25] S. H. White and U. M. Twardoch, *Electrochim. Acta* **27** (1982) 1599.

[26] S. H. White and U. M. Twardoch, *J. Electrochem. Soc.* **134** (1987) 1080.

[27] S. H. White and U. M. Twardoch, *Electrochim. Acta* **29** (1984) 349.

[28] S. H. White in 'Molten Salt Techniques', Vol. 1 (edited by D. G. Lovering and R. J. Gale) Plenum (1983) p. 19.

[29] C. R. Wolfe and R. D. Caton, *Anal. Chem.* **43** (1971) 663.

[30] M. D. Ingram, B. Baron and G. J. Janz, *Electrochim. Acta* **11** (1966) 1629.

[31] B. Andersen, Ph.D. Thesis, The Technical University of Denmark, 1975.

[32] J. O'M Bockris and A. K. N. Reddy, 'Modern Electrochemistry', Vol. 1, McDonald, London (1970).

[33] S. H. White and U. M. Twardoch, Abstract No. 518, ECS meeting, Las Vegas.

[34] M. S. Shuman, *Analyt. Chem.* **41** (1969) 142.

[35] R. S. Nicholson, *Analyt. Chem.* **38** (1966) 1406.

[36] P. L. Spedding and R. Mills, *J. Electrochem. Soc.* **112** (1965) 594.

[37] P. L. Spedding and R. Mills, *J. Electrochem. Soc.* **113** (1966) 599.

[38] G. J. Janz, 'Molten Salts Handbook', Academic Press, New York (1967) pp. 349–355.

[39] D. Inman, Dj Jovanovic and S. H. White, *J. Electroanal. Chem.* **43** (1973) 37.

[40] G. J. Janz, C. B. Allen, N. P. Bansal, R. M. Murphy and R. P. T. Tomkins, 'Physical Properties Data Compilations Relevant to Energy Storage', NSRDS. NBS 61 Part II (1979).